Compact tunable laser source emitting in the LWIR for standoff gas sensing

Marine Favier, Basile Faure, Grégoire Souhaité, Jean-Michel Melkonian, Antoine Godard, Myriam Raybaut, Arnaud Grisard, Eric Lallier

COMPACT TUNABLE LASER SOURCE EMITTING IN THE LWIR FOR STANDOFF GAS SENSING

Marine Favier[(1)], Basile Faure[(1)], Grégoire Souhaité[(1)], Jean-Michel Melkonian[(2)], Antoine Godard[(2)], Myriam Raybaut[(2)], Arnaud Grisard[(3)], Eric Lallier[(3)]

(1) Teem Photonics, 61 Chemin du Vieux Chêne, Innovallée, 38240 Meylan, France, m.favier@teemphotonics.com
(2) ONERA, DPHY, Université Paris Saclay, F-91123 Palaiseau, France
(3) Thales Research & Technology, 1 Avenue Augustin Fresnel, 91767 Palaiseau, France

KEYWORDS: laser, nanosecond, long infrared, single mode, optical parametric oscillation

ABSTRACT:
Tunable coherent sources emitting in the Long Wave Infra Red (LWIR), between 7 and 14 µm can be used in defense application such as standoff detection of hazardous gas and chemical warfare agents. In a previous ANR/DGA project called MUSTARD, we demonstrated, in the laboratory, a single longitudinal mode optical parametric oscillator (OPO) emitting in the 8 – 11 µm domain. This OPO used a quasi-phase-matched (QPM) GaAs crystal, pumped by a Tm:YAP microlaser [1] [2]. Now we present the development, as part of the DGA SPICE project, of a compact (~600 cm² footprint) and robust industrial prototype (Figure 1) based on the same architecture including an original setup for real time measurement of the emitted wavelength.

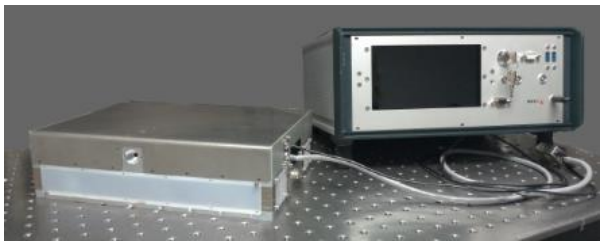

Figure 1: LWIR source prototype and its controler

1. CONTEXT

Non-intrusive, standoff detection of hazardous chemical species, such as chemical warfare agents (CWAs), toxic industrial chemicals (TICs), and explosives precursors is an important issue for both civilian and military applications. Among the existing methods, laser-infrared spectrometry is promising as it provides non-intrusive and selective standoff detection of chemicals. Active detection systems based on infrared laser spectroscopy, such as differential absorption lidars (DIALs), have already proved to provide the best performances to detect atmospheric trace gases, with detection ranges from a few tens of meters to several kilometers. However, for most of the species involved in defense and security applications, the strongest non overlapping absorption lines are located in the longwave infrared (LWIR) range between 7.5 µm and 12 µm. Indeed, this spectral window not only gathers fundamental rovibrational lines but shows low absorption of water molecules which allows light to propagate over long distance.

In the context of standoff detection by infrared spectroscopy, optical coherent sources with narrow spectral linewidth and broad wavelength tunability are attractive to enable selective multi-species detection. At long wavelengths, solid-state materials suitable as laser active ion hosts are scarce, as they usually present strong multiphonon absorption. Only two types of laser technologies are available for direct emission in the LWIR : the CO_2 gas laser and the quantum cascade laser (QCL). Until the advent of QCLs, the CO_2 laser has been the only coherent source available in the LWIR with a significant energy, and has been extensively used in lidar emitters for standoff detection of chemicals. Several emitters delivering more than 100 mJ have been developed, mainly for detection of CWAs and TICs. Energies above 1 J have been demonstrated in operational lidars [3-4].
More recently, the CO_2 laser has been used for standoff detection of explosives. However, the restricted tunability still prevents addressing the strongest absorption bands of most gases, and sometimes precludes detection of the species at all, sulfur mustard for instance. QCLs are now the workhorses of many spectroscopy and local gas sensing experiments. However due to their limited peak power, standoff detection with QCL is currently limited to ranges of a few tens of meters.

To overcome these limitations, another solution is to use second-order nonlinear optics to archieve down-conversion to the LWIR. For instance, optical parametric oscillator are well suited for standoff detection of chemicals because they provide peak powers in the kilowatt range, greater wavelength tunability compared to QCLs and CO_2 lasers and good optical quantum efficiencies (typically around 30% with Gaussian beams). Most of previous research studies focused on pumping crystals such

as $AgGaSe_2$, $BaGa_4S_7$, $ZnGeP_2$, CdSe and orientation-patterned GaAs (OP-GaAs) where wavelength tunability can reach a few micrometers in the LWIR. Among these crystals, GaAs is one of the most interesting for parametric frequency conversion thanks to the following features : a broad transparency window ranging from 0.9 to 17 µm, a high second order nonlinear susceptibility (d_{14} = 90 pm V^{-1}) [5], and excellent mechanical and thermal properties. GaAs is optically isotropic, precluding birefringent phase-matching, but it is free from spatial walk-off which usually limits the maximum usable length.

The OPO is based on the doubly-resonant nested cavity OPO (NesCopo) scheme that enables to deliver a pulsed single-longitudinal-mode emission without using any intra-cavity optical elements or resorting to injection seeding. This approach was previously used with PPLN crystals and applied to the detection of various gases at wavelengths spanning from 2 to 4.2µm [6-8]. The concept was extended in the laboratory to the LWIR with a QPM GaAs [1], as part of the DGA MUSTARD project and our group reported on the first nanosecond OP-GaAs OPO emitting a tunable single frequency radiation in the LWIR and showed its potential for standoff detection. Here, we present the following of the project, in the frame of the DGA RAPID SPICE project, to produce a compact tunable source.
First, we'll present the principle of this OPO and how single-frequency operation is verified and maintened over the tunability range. Then, we'll present the performances of the protoype and the measured tunability in the 8 µm range.

2. SINGLE FREQUENCY TUNABLE 8-11 µM LASER SOURCE

2.1 Overview of the source

The overall architecture of the source is presented in Figure 2. The LWIR source is composed of three main parts: a 2 µm pump microlaser source; a nanosecond OPO, designed to deliver single longitudinal emission; and a Sum Frequency Generation (SFG) conversion scheme, for LWIR emission wavelength measurement. Given the difficulty of accurately measuring wavelengths in these emission ranges, we introduce in the package a real time measurement of the emitted wavelength after nonlinear conversion to reach 1 µm range.

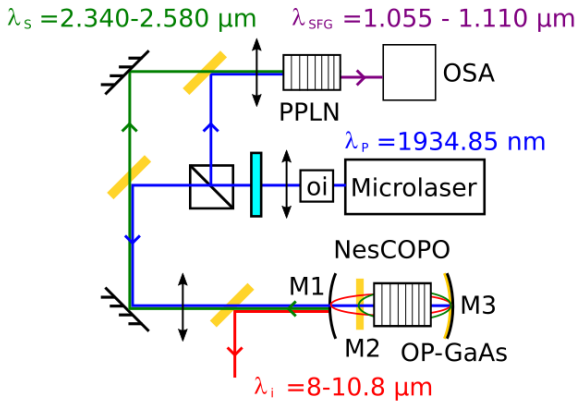

Figure 2: Architecture of the LWIR source.

2.2 Single frequency 1.94 µm pump laser

A single-frequency pulsed Tm:Yap microlaser, emitting at 1934.85 nm was specially engineered for this application [9]. The laser rod is a 4 mm long 3% at Tm/Yap, cut along the a-axis in the Pnma space group. To limit the number of elements in the cavity the input mirror has been deposited on one of its facet (HT@ 795 nm, HR@ 1940 nm), and the second facet is antireflection coated at both the pump and laser wavelengths. The laser crystal is pumped by a 3W C-Mount diode, emitting near 790 nm, mounted on a Peltier stage to better match the peak absorption of the Tm:Yap crystal. Passively Q-switched operation is obtained inserting a Cr:ZnSe saturable absorber with 96% transmission. A pump modulation scheme was implemented to reduce the jitter of the laser and facilitate single-longitudinal-mode operation. For 2.4 W of pump power modulated at 300 Hz, the microlaser delivers pulses of 110 µJ with 36 ns pulse duration, corresponding to ~3 kW peak power. The laser is mounted in an industrial and compact packaging (60 mm x 139 mm x 47 mm) that weights around 500 g (Figure 3). Moreover, it comprises an optical isolator inserted in the case to protect the laser from optical feedback, a collimating lens and a filter to absorb the residual pump diode laser.

Figure 3: 1.94 µm pump microlaser

These three elements introduces 30% of losses. When the laser is closed, the energy impulsion is 77 µJ. The output beam diameter ($1/e^2$) is 1300 µm. Longitudinal single mode operation of

the 3 GHz free spectral range (FSR) cavity was verified using a Fabry Perrot interferometer of 10 GHz FSR operating in the 2 µm range.

2.3 Nested OPO

The OPO mentioned as NesCOPO consists of a dual-cavity doubly resonant OPO where the signal and the idler cavity length are controlled separately, presented in Figure 4. In this architecture the two wavelengths produced by the non linear crystal oscillate in separated cavities. This approach leads to single-longitudinal-mode operation for an adequate differentiation of the cavity lengths because only a single exact coincidence of signal and idler modes can be obtained within all the parametric gain bandwidth, as illustrated in Figure 5.

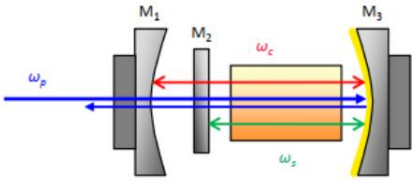

Figure 4: Illustration of the NesCOPO doubly resonant cavities:

The idler cavity is made of a first mirror M1 with a radius of curvature of 20 mm, reflecting the idler with an average reflectivity of 85% in the 8-11 µm range and transmitting the pump and the signal. The second idler mirror is a gold-coated mirror with a radius of curvature of 50 mm. The signal cavity is made of a plane mirror M2 that reflects 98% of the signal wave and transmits the other waves, and of M3 as the second mirror. M3 also reflects the pump wave, which lowers the oscillation threshold. The OP-GaAs crystal is inserted between M2 and M3 in a temperature-controlled oven. The signal and idler cavities free spectral ranges are both close to 4 GHz. Mirrors M1 and M3 are mounted on piezo-electric transducers (PZTs) to finely adjust both cavity lengths.

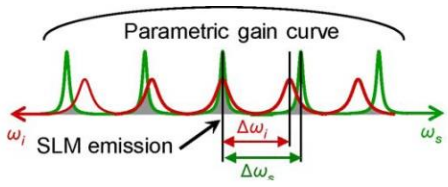

Figure 5: Giordmaine and Miller diagram. Illustration of mode selection in the NesCOPO. The signal and idler frequency axes are oriented in opposite directions to fulfill energy conservation.

2.4 GaAs crystals

We used two OP-GaAs samples which were grown during precedent project. Their characteristics are presented in Table 1. They are periodically oriented and grown by epitaxy in vapor phase [10]. In this method, two layers of GaAs with opposite crystallographic directions [001] and [00-1] are superimposed on a GaAs wafer. The domain periods and duty cycles are defined by photolithography, and the patterned template is etched to reveal the grating. Finally, the material grows on about 500 µm by epitaxy in vapor phase. The crystal's facets are then anti-reflection coated for the pump, signal and idler waves. The surface damage threshold was measured to be approximately 0.6 J.cm^{-2} at 2 µm for anti-reflection coated crystals.

Table 1: Specification of the OP-GaAs crystals

Crystal	M22 (multi-tracks)			M28
	Λ_1	Λ_2	Λ_3	Λ_4
Length (mm)	10			6
QPM period (µm)	63.6	64.8	66	72.6
Idler (µm) 20°C-100°C	7.7-8.2	8-8.6	8.3-8.9	10.3-11.2

Pictures of these crystals are shown in Figure 6. Idler emission in the ~8 to 11 µm range is possible by selecting the crystal and track.

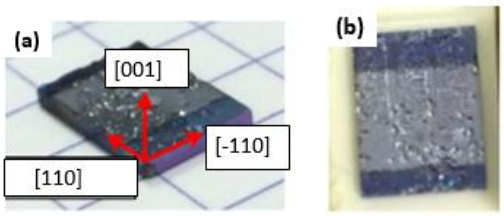

Figure 6: Pictures of the GaAs crystals

At first order and far from degeneracy the theoretical double-pass gain bandwidth is given by:

Eq. 1

$$\Delta s = \frac{1}{2L.(ng,s - ng,i)}$$

Where L is the crystal length, ng stands for the group index, and the subscripts s, I for the sigal and idler waves respectively. In our case, the theoretical gain bandwidth is 8.4 cm^{-1} for a 10 mm long OP-GaAs crystal using the group index given in [5]. Without any spectral selection mechanism, as in a singly resonant OPO, there would be approximately 65 longitudinal modes that could oscillate under the gain bandwidth with a cavity free spectral range of 4 GHz.

2.5 Sum Frequency Generation (SFG) for idler wavelength real time measurement

The emitted wavelength is measured thanks to a SFG scheme impliying the signal wave and the

remaining pump. The emission of signals extends from 2.3 µm to 2.5 µm. The back converted SFG signal extends then from 1.06 µm to 1.1 µm which enables the wavelength measurement with a compact and affordable silicon based optical spectrum analyser. Idler signal wavelength is deduced from the SFG wavelength measurement, knowing the pump wavelength. The frequency of the idler, signal, pump are linked with the conservation of energy.

Eq. 2 $$\nu P = \nu S + \nu C$$

While the sum frequency signal are linked with :

Eq. 3 $$\nu SFG = \nu S + \nu P$$

Combining these two equations leads to

Eq. 4 $$\nu S = \nu SFG - \nu SHG/2$$

Eq. 5 $$\nu C = \nu SHG - \nu SFG$$

Experimentally, the signal wave is directed toward a periodically poled lithium niobate (PPLN) crystal and focused with a waist of 75 µm (radius $1/e^2$). The PPLN is 20 mm long and has a chirped period, extended from 30.76 µm to 35.24 µm.

The optical spectrum analyser (OSA) has a fixed window of operation of 10 nm with 6.8 GHz resolution.

Figure 7 shows the SFG spectrum obtained when the mirror has been tuned to sweep all the modes of the crystal gain bandwidth. The crystal was operating at ambiant temperature around 20°C. The isolated peak at 1094 nm. corresponds to parasitic Second Harmonic Generation (SHG) of the pump laser which is folded in the same spectral region than the SFG peaks because the OSA works with fixed element.

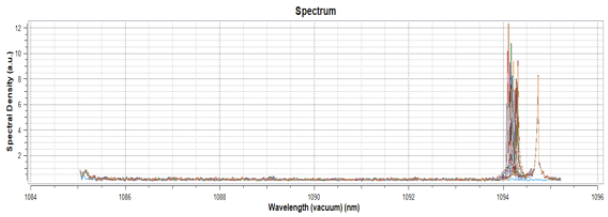

Figure 7: SFG spectrum measured with the silicon OSA when the mirror has been tuned to sweep all the modes of the crystal gain bandwidth

A peak detection algorithm has been implemented to follow the wavelength during time. It consists in a pre-detection of a peak using least square polynomial, followed by a non linear least square fitting with lorentzian function. This second step enables to go below the OSA spectral resolution.

3. LWIR SOURCE CHARACTERIZATION

In the following, we present the results obtained for the crystal M28 with period of 66 µm. We focused our effort on this crystal because it enables to reach wavelength of the absorption of Mustard gas.

3.1 Output power emission

The LWIR laser source emits single longitudinal pulses up to 200 nJ. Figure 8 shows the measured idler energy as a function of the incident pump energy for crystal M28. Pumping more thant three to four times above threshold is not advised as it can lead to multimode operation due to less efficient Vernier spectral filtering of the side-modes.

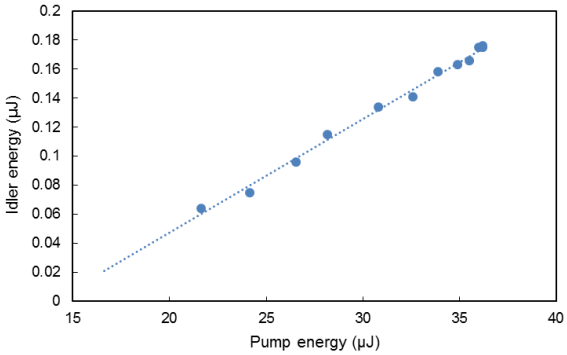

Figure 8: Idler energy at 8 µm as function of incident pump energy

Figure 9 shows the temporal pulse profiles of the incident and depleted pump as well as the idler profile. We determined an average pump depletion of 15% with a pump energy four times above thereshold.

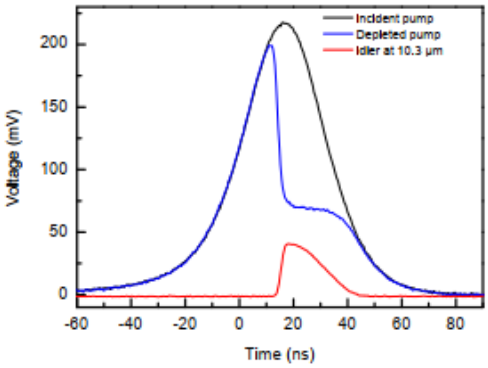

Figure 9: Temporal pulse profiles of incident pump (black line), depleted pumpe (blue line) and idler (red line)

3.2 Fine wavelength tuning with cavity length

As explained in section 2.3, single frequency operation is achieved when the dissociation parameter $\Delta L/L$ is adjusted to avoid both multiple exact coincidence and clusters of modes under the gain bandwidth. Experimentally, we mechanically

adjust the idler cavity length while recording frequency emission when the piezzo mounted on M1 tune the idler bandwidth.

The mechanical dissociation is found to be 1.6 %. Figure 10 shows the frequency of the SFG signal recorded with a 100 V triangle signal applied on the piezzo. In the figure, dashed lined corresponds to inversion of the piezzo ramp. The record starts with positive ramp. The cavity length tuning by piezo element leads to a fine tuning of idler wavelength capacity from ~8.38 µm to 8.42 µm with one specific track and at fixed temperature of 30°C.

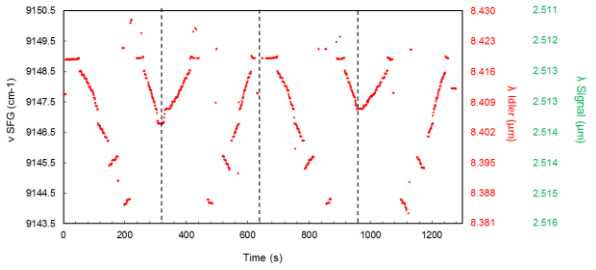

Figure 10: SFG signal frequency during idler cavity length scanning. Deduced signal and idler frequency are shown in left axis

When zooming on the emission wavelength (Figure 11), we see that we can measure, and thus control, wavelength shift corresponding to the free spectral range of the cavity.

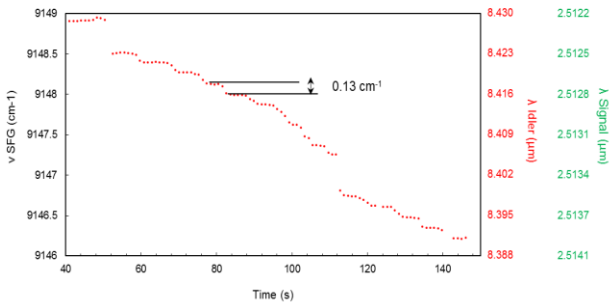

Figure 11 : Close up of SFG signal frequency during cavity length scanning. Deduced signal and idler frequency are shown in left axis

Holes in the emission wavelength have been recorded. They are attributed to parasitic fringes.

3.3 Temperature tuning

The crystal temperature has been changed to shift the gain bandwidth toward higher idler central wavelength. Figure shows this shift in wavelength. We archieved a tunability from 8.356 µm to 8.484 µm by heating the crystal up to 40°C which corresponds to a rate of 6.4 nm/°C.

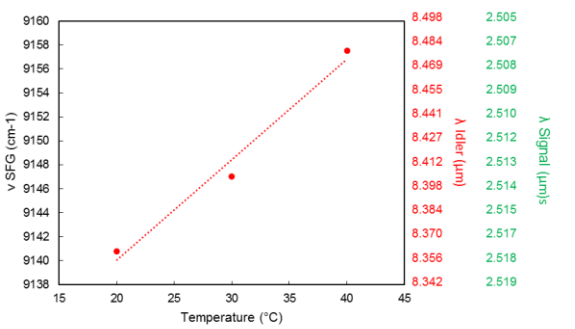

Figure 12 SFG signal frequency during elevation of the temperature crystal. Deduced signal and idler frequency are shown in left axis.

4. CONCLUSION

We have presented a compact industrial prototype of LWIR source that can emit in the 8 to 11 µm region. The source was designed to be used in real environmental conditions and is considered to have an industrialization level of TRL 5. It is based on doubly resonant cavity OPO where the frequency conversion is realized through an OP-GaAs crystal pumped by a 2 µm microlaser.

The OPO is designed to operate on a single longitudinal mode up to four times above the operation threshold (10µJ). It emits an idler wave in the 8-11 µm range with an energy of more that 100 nJ. Moreover, the source contains in its package an original sum frequency scheme involving the signal wave (2.3 µm – 2.5 µm) and the 1.94 µm pump. To enables real wavelength measurement with a compact industrial OSA in the 1 µm region. Control of the wavelength from 8.7 µm to 8.4 µm with a precision of 6 GHz has been obtained. An electronic controller was designed along with the optical head to fully automate the control of the wavelength emission of the OPO.

The next steps will be to pump the OPO with a tunable laser around 2 µm, to amplify the idler energy using parametric amplification in GaAs crystals, and perform standoff detection of gases using a laboratory lidar setup.

5. ACKNOWLEDGEMENT

We acknowledge Direction Générale de l'Armement (DGA) for funding through the RAPID program (convention RAPID n°172906032-172906033-172906034).

6. REFERENCES

1. Q. Clément, J.-M. Melkonian, J.-B. Dherbecourt, M. Raybaut, A. Grisard, E. Lallier, B. Gérard, B. Faure, G. Souhaité, and A. Godard, **"**Longwave infrared, single-frequency, tunable, pulsed optical parametric oscillator based on orientation-patterned GaAs for gas sensing**"**, *Optics Letter* 40, 2676 (2015)

2. Armougom, J., Melkonian, JM., Dherbecourt, JB. et al. « A narrowband infrared source based on orientation-patterned GaAs for standoff detection of chemicals » Appl. Phys. B (2018) 124: 133.

3. Adam P., Duvent Jean-Louis, and Steven W.Gotoff « Detection and reconnaissance of pollutant clouds by CO2 lidar (MIRELA) », Proc SPIE 3127, Application of Lidar to Current Atmospheric Topics II, (31 october 1997);

4. Clinton B. Carlisle, Jan E. van der Laan, Lewis W. Carr, Philippe Adam, and Jean-Pierre Chiaroni, "CO_2 laser-based differential absorption lidar system for range-resolved and long-range detection of chemical vapor plumes," Appl. Opt. 34, 6187-6200 (1995)

5. T. Skauli, K. L. Vodopyanov, T. J. Pinguet, A. Schober, O. Levi, L. A. Eyres, M. M. Fejer, J. S. Harris, B. Gerard, L. Becouarn, E. Lallier, and G. Arisholm, "Measurement of the nonlinear coefficient of orientation-patterned GaAs and demonstration of highly efficient second-harmonic generation," Opt. Lett. 27, 628-630 (2002)

6. B. Hardy, A. Berrou, S. Guilbaud, M. Raybaut, A. Godard, and M. Lefebvre, "Compact, single-frequency, doubly resonant optical parametric oscillator pumped in an achromatic phase-adapted double-pass geometry," Opt. Lett. 36, 678-680 (2011)

7. B. Hardy, M. Raybaut, J.-B. Dherbecourt, J.-M. Melkonian, A. Godard, A. K. Mohamed, and M. Lefebvre, "Vernier frequency sampling: a new tuning approach in spectroscopy application to multi-wavelength integrated path DIAL", *Appl. Phys. B* **107**(3), 643-647 (2012)

8. J. Barrientos Barria, D. Mammez, E. Cadiou, J.-B. Dherbecourt, M. Raybaut, T. Schmid, A. Bresson, J.-M. Melkonian, A. Godard, J. Pelon, and M. Lefebvre, "Multispecies high-energy emitter for CO_2, CH_4, and H_2O monitoring in the 2 µm range", *Opt. Lett.* **39**(23), 6719-6722 (2014)

9. A. Grisard, B. Faure, G. Souhaité and E. Lallier, "High energy single frequency passively Q-switched 2-micron microlaser in thulium-doped yttrium aluminium perovskite", paper ATu2A.39 in ASSL, OSA (2014)

10. Arnaud Grisard, Eric Lallier, and Bruno Gérard, "Quasi-phase-matched gallium arsenide for versatile mid-infrared frequency conversion," Opt. Mater. Express 2, 1020-1025 (2012)²